

## Accepted Manuscript

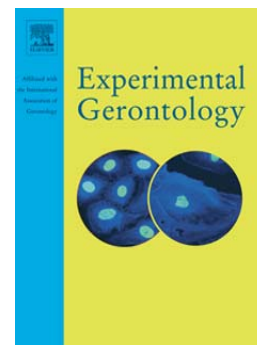
Neuroprotective role of intermittent fasting in senescence-accelerated mice P8 (SAMP8)

M. Tajés, J. Gutierrez-Cuesta, J. Folch, D. Ortuño-Sahagun, E. Verdaguier, A. Jiménez, F. Junyent, A. Lau, A. Camins, M. Pallàs

PII: S0531-5565(10)00188-9  
DOI: doi: [10.1016/j.exger.2010.04.010](https://doi.org/10.1016/j.exger.2010.04.010)  
Reference: EXG 8747

To appear in: *Experimental Gerontology*

Received date: 25 December 2009  
Revised date: 23 April 2010  
Accepted date: 29 April 2010



Please cite this article as: Tajés, M., Gutierrez-Cuesta, J., Folch, J., Ortuño-Sahagun, D., Verdaguier, E., Jiménez, A., Junyent, F., Lau, A., Camins, A., Pallàs, M., Neuroprotective role of intermittent fasting in senescence-accelerated mice P8 (SAMP8), *Experimental Gerontology* (2010), doi: [10.1016/j.exger.2010.04.010](https://doi.org/10.1016/j.exger.2010.04.010)

This is a PDF file of an unedited manuscript that has been accepted for publication. As a service to our customers we are providing this early version of the manuscript. The manuscript will undergo copyediting, typesetting, and review of the resulting proof before it is published in its final form. Please note that during the production process errors may be discovered which could affect the content, and all legal disclaimers that apply to the journal pertain.

**Neuroprotective role of intermittent fasting in senescence-accelerated mice P8 (SAMP8)**

M. Tajés<sup>1,2</sup>, J. Gutierrez-Cuesta<sup>1,2</sup>, J. Folch<sup>2,3</sup>, D. Ortuño-Sahagun<sup>4</sup>, E. Verdaguer<sup>1,2</sup>, A. Jiménez<sup>1,2</sup>, F. Junyent<sup>2,3</sup>, A. Lau<sup>5</sup>, A. Camins<sup>1,2</sup> and M. Pallàs<sup>1,2</sup>

<sup>1</sup>Unitat de Farmacologia i Farmacognòsia Facultat de Farmàcia, Institut de Biomedicina (IBUB), Universitat de Barcelona. Nucli Universitari de Pedralbes. 08028 Barcelona, Spain.

<sup>2</sup>Centros de Investigación Biomédica en Red de Enfermedades Neurodegenerativas (CIBERNED).

<sup>3</sup> Unitat de Bioquímica, Facultat de Medicina i Ciències de la Salut, Universitat Rovira i Virgili. C./ St. Llorenç 21 43201 Reus (Tarragona), Spain

<sup>4</sup>Laboratorio de Desarrollo y Regeneración Neural, Instituto de Neurobiología, Departamento de Biología Celular y Molecular, C.U.C.B.A, Universidad de Guadalajara, Guadalajara, Jalisco, Mexico.

<sup>5</sup>Department of Neurosciences, Case Western Reserve University, Cleveland, Ohio, USA

Correspondence to: Mercè Pallàs, PhD

Unitat de Farmacologia i Farmacognòsia Facultat de Farmàcia

Universitat de Barcelona. Nucli Universitari de Pedralbes. E-08028 Barcelona, Spain

e-mail: pallas@ub.edu

**ABSTRACT**

Dietary interventions have been proposed as way to increase lifespan and improve health. The senescence-accelerated prone 8 (SAMP8) mice have a shorter lifespan and show alterations in the central nervous system. Moreover, this mouse strain shows decreased sirtuin 1 protein expression and elevated expression of the acetylated targets NFκB and FoxO1, which are implicated in transcriptional control of key genes in cell proliferation and cell survival, in reference to control strain, SAMR1. After eight weeks of intermittent fasting, sirtuin 1 protein expression was recovered in SAMP8. This recovery was accompanied by a reduction in the two acetylated targets. Furthermore, SAMP8 showed a lower protein expression of BDNF and HSP70 while intermittent fasting re-established normal values. The activation of JNK and FoxO1 were also reduced in SAMP8 mice subjected to an IF regimen, compared with control SAMP8. Our findings provide new insights into the participation of sirtuin 1 in ageing and point to a potential novel application of this enzyme to prevent frailty due to ageing processes in the brain.

**Key words:** ageing, neurodegeneration, NFκB, ADAM10, BDNF, sirtuin 1

## INTRODUCTION

A reduced calorie intake extends the lifespan and increases resistance to age-related diseases in rodents and monkeys, as well as improving the health of overweight humans (Martin et al., 2006) by enhancing cardiovascular and brain functions and decreasing several risk factors for coronary artery disease and stroke. For example, a reduced calorie diet lowers blood pressure and enhances insulin sensitivity. In addition, rodents on a low calorie diet show improved cardiovascular stress adaptation and increased heart rate variability. Moreover, experimental rodent models of myocardial infarction and stroke on an intermittent fasting (IF) regimen exhibit increased resistance of heart and brain cells to ischemic injury. The beneficial effects of IF and caloric restriction (CR) result from at least two mechanisms, namely reduced oxidative damage and increased cellular stress resistance (Calabrese et al., 2008). In the epidemiology of neurodegenerative diseases, the incidence of sporadic Parkinson's disease (PD) and Alzheimer's disease (AD) is correlated with multiple genetic factors, diet and social behavior (Mattson et al., 2002). High calorie diets are associated with the risk of AD, and it has been proposed that a low calorie diet may afford protection against PD and AD (Mattson, 2003). A possible link between CR and AD was proposed after observations of the potential benefits of sirtuin 1 activation on AD symptoms and progression (Westphal et al., 2007).

Sirtuin 1 is an NAD-dependent deacetylase that not only deacetylates histone but also several proteins and substrates modifying its action or activity. Amongst the non-histone cellular substrates of sirtuin 1 are the tumor suppressor p53, the transcription factor NF- $\kappa$ B and the FOXO family of transcription factors. All the above are involved in transcriptional control of key genes in cell proliferation and cell survival. Sirtuin 1 also deacetylates nuclear receptor peroxisome-proliferator activated receptor- $\gamma$  (PPAR $\gamma$ ) and its transcriptional co-activator PPARc coactivator- $\alpha$  (PGC- $\alpha$ ), which regulate a wide range of metabolic activities in muscle, adipose tissues and liver (Rodgers et al., 2005; Salminen et al., 2008; Smith, 2002). Recent findings also suggest that some of the beneficial effects of IF on the cardiovascular system and the brain are mediated by brain-derived neurotrophic factor signalling (BDNF) in the brain (Duan et al., 2001). In reference to implication of sirtuin 1 in neurodegeneration, SIRT1 may regulate aging and neurodegenerative processes, including protein aggregation, stress responses

(FOXO,p53,Ku70), mitochondrial dysfunction (PGC-1 $\alpha$ ), and inflammation (NF- $\kappa$ B and LXR). Considerable evidence indicates that the sirtuin 1 pathway regulates cell survival mechanisms and that it rescues proteins in a number of neurodegenerative conditions (Hippkiss, 2007). For example, deacetylation of FoxO1 by sirtuin 1 promotes the expression of p27/kip1 and manganese superoxide dismutase. This observation implicates sirtuin 1 in decreased oxidative stress and in cell cycle control (Wang et al., 2007). Qin et al, 2006 report that the predicted attenuation of  $\beta$ -amyloid content in the brain during CR can be reproduced in mouse neurons *in vitro* by manipulating cellular sirtuin 1 expression/activity through mechanisms involving the regulation of the serine/threonine Rho kinase ROCK1, known in part for its role in the inhibition of the non-amyloidogenic  $\alpha$ -secretase (ADAM10) processing of the amyloid precursor protein.

Senescence-accelerated mice (SAM) were originally generated from AKR/J mice (Takeda, 1999). SAMP, Senescence-accelerated prone mice, strains show normal development and maturity of reproductive function, followed by an early manifestation of senescence-related phenotypes indicative of accelerated ageing, including loss of hair, lordokyphosis, periophthalmic disorders, loss of activity and shortened life. Early changes in SAMP8 (between 3 and 5 months old) have been reported, thereby confirming the accelerated senescence of this strain (Canudas et al., 2005;Tajes et al., 2008). The long-lived mice SAMR1, littermates of age-accelerated mice, do not show senescence-related phenotypes and are commonly used as a control strain. It has been suggested that restriction of calorie intake is crucial for the prevention of learning and memory deficits in different animal models (Komatsu et al., 2008).

Collectively, data indicate that long-term reductions in energy intake during adult life protect the brain against diseases associated with ageing. Thus, energy restriction should be considered, together with exercise and cognitive enrichment, as an approach for reducing the risk of AD. A better understanding of the cellular and molecular mechanisms by which reduced calorie intake affects brain cells may lead to novel preventive and therapeutic strategies for extending life expectancy and for tackling neurodegenerative diseases. Here we studied a murine model of senescence (SAMP8) under IF to delineate some of the pathways activated by this dietary strategy and elucidate their possible role in the prevention of senescence-related brain impairment

and the onset of AD. The pathway of sirtuin 1, a critical signalling cascade involved in cell proliferation and survival, was of the main interest.

## Materials and methods

### Mice

Weaned male SAMP8 and senescence accelerated-resistant 1 (SAMR1) mice were housed under controlled temperature and light conditions (21–24 °C, 12-hour (h) light/12-h dark cycle) in an animal facility at the University of Barcelona. Animal care and experimental procedures were performed in accordance with the Guidelines for Animal Experimentation established by the “Generalitat de Catalunya” (Spain), with the approval of the University of Barcelona’s Animal Care and Use Committee (CEEA-UB). Four-week-old mice were divided into 4 groups of 10 males per group. The groups were assigned to dietary regimens as follows: SAMR1 ad libitum (SAMR1); SAMP8 ad libitum (SAMP8); SAMR1 intermittent fasting (IF-SAMR1); and SAMP8 intermittent fasting (IF-SAMP8). All mice ate standard mouse food pellets (Harlan standard diet). Mice on the IF diet were deprived of food for 24 h every other day. During all procedures, food intake and body weight was monitored.

### Brain isolation and Western blot analysis

After 8 weeks of the IF protocol, mice were killed by decapitation between 9:00 and 12:00 h after a feeding day. The brain was immediately removed and dissected into cortex and hippocampus. Each brain part was frozen in powdered dry ice and maintained at –80 °C until use.

Tissues were homogenized in lysis buffer containing protease inhibitors (Cocktail II, Sigma, St Louis, MO, USA). The protein concentration in the tissue samples was determined using the BCA protein assay kit (Pierce, Rockford, IL, USA). 20 micrograms of protein was separated by SDS–PAGE (8–12%) and transferred to nitrocellulose membranes. The membranes were blocked in 5% non-fat milk for 1 h at room temperature followed by an overnight incubation at 4 °C with antibodies against sirtuin 1, p-FoxO1, FoxO1, p-GSK3 $\beta$  Tyr<sup>216</sup>, GSK3 $\beta$ , p-JNK, JNK, BDNF (1:1000, from Cell Signaling, Beverly, MA, USA), p-tau Ser<sup>199</sup> (1:1000; Biosource-Invitrogen Corp., Carlsbad, USA), HSP70 (1:1000, Stressgen, San Diego, CA, USA), ADAM 10

(1:1000 from ABCAM, Cambridge, UK) and  $\beta$ -actin (1:20000 in blocking buffer, from Neomarkers, Fremont, CA, USA). The membranes were washed and incubated with secondary antibodies for 1 h at room temperature. Protein bands were visualized using a chemiluminescence detection kit (Amersham Corp., Arlington Heights, IL, USA). Band intensities were quantified by densitometric analysis, and values were normalized to actin expression.

### **Co-immunoprecipitation**

For the co-immunoprecipitation experiment, total protein (50  $\mu$ g) was brought to a final volume of 0.5 mL with PBS + 2% BSA and incubated with 4  $\mu$ g of anti-FoxO1 total for 6 h at 4°C. Immunocomplexes were captured by incubating the samples with protein A-agarose suspension overnight at 4°C on a rocker platform. After microcentrifugation, the pellet was washed in 60  $\mu$ l of SDS-PAGE sample buffer and boiled for 5 min at 100°C. An aliquot of the supernatant was subjected to electrophoresis in 10% SDS-PAGE and immunoblotted with antibody against acetyl-lysine (1:1000, from Cell Signaling).

### **Extraction and Quantification of Total RNA**

Total RNA isolation was carried out by means of the NucleoSpin® RNA II kit, following the manufacturer's instructions. Briefly, cell culture medium was removed and cells rinsed with PBS and lysed directly in the culture dish by adding lysis buffer containing  $\beta$  mercaptoethanol. For each preparation, one NucleoSpin® RNA II column Macherey-Nagel (Macherey-Nagel GmbH & Co. KG, Düren, Germany) was placed in a 2-mL centrifuge tube and the lysate was loaded. After centrifugation, 30 s at 8,000g, the column was desalted and loaded with 95  $\mu$ L of DNase I reaction mixture. After 15 min of digestion at room temperature, the RNA was eluted from the column and recovered in 50  $\mu$ l H<sub>2</sub>O (RNase-free). RNA content in the samples was measured at 260 nm and purity of the samples was determined by the A260/280 ratio and through ethidium bromide fluorescence of RNA resolved in 1% agarose gels. Samples were also tested in a bioanalyzer 2100B (Agilent Technologies, Santa Clara CA, USA) to determine the RNA Integrity Number (RIN).

### **Probe Preparation and Hybridization to low density arrays**

The RNA used for the hybridization experiments was purified from a pool of brains taken from four mice from each experimental group. For cDNA synthesis, 10  $\mu$ g of

total RNA was used as a template, incorporating dUTP-Cy3 or dUTP-Cy5 with the CyScribe First-Strand cDNA labeling kit (Amersham Corp.). Incorporation of the fluorophore was analyzed by evaluating absorbance at 555 nm for Cy3 and at 655 nm for Cy5. Array hybridization and washing was performed with a Lucidea Slide Pro (Amersham Corp.) system. Equal amounts of labeled cDNA were hybridized for 14 h at 42°C to the oligo mice arrays in UniHyb hybridization solution (TeleChem International, Inc., Sunnyvale, CA, USA).

### **Data Acquisition and Analysis of Array Images**

Hybridization data were obtained by using a scanner GenePix 4000B (Axon) and microarray data analysis was performed with the GenArise software, developed by the Computing Unit at the Cellular Physiology Institute of the UNAM (Gómez-Mayen, 2006), as previously described (Rojas-Mayorquin et al., 2008). The software identifies differentially expressed genes by calculating an intensity-dependent z-score. By applying these criteria, the elements with a z-score > 1.5 standard deviations are genes likely to be differentially expressed.

### **Reverse transcriptase-PCR**

Total RNA was extracted from hippocampus tissue samples using Trizol reagent, following the manufacturer's instructions. Isolated RNA was treated with amplification grade DNase I for 7 min at room temperature to remove contaminant genomic DNA. First-strand cDNA was reverse transcribed from 2 µg of total RNA using a First-Strand Synthesis System kit from Invitrogen. β-actin primers were designed to cross a large expanse of intronic sequence between exons 2 and 3 of the mouse gene. Primer non-reactivity with contaminating genomic DNA was tested by including controls that omitted the reverse transcriptase enzyme from the cDNA synthesis reaction (RT-negative controls). The lack of primer dimerization or non-specific PCR product bands was also tested.

### **Real-time PCR quantification using SYBR Green**

Quantification of relative gene expression was performed by real-time quantitative PCR, using the ABI PRISM 7700 Sequence Detection System (Applied Biosystems, Foster City, CA, USA). Real-time PCR was carried out using a SYBR Green PCR kit. Quantitative PCR was carried out using the following thermal cycling program. Stage 1



was undertaken at 95°C for 15 min while stage 2 consisted of the following three steps repeated for 40 cycles: 95°C for 15 s; 60 °C for 30 s; and 72°C for 30 s. Relative mRNA expression was calculated by the standard curve method. In brief,  $\beta$ -actin and target gene amplifications were run in separate tubes. Standard curves were obtained for all genes by using decreasing amounts of cDNA template. PCR reactions were performed in duplicate for standard curves whereas samples were tested in triplicate, at a final volume of 25  $\mu$ l in all cases. For each cDNA template, the cycle threshold (Ct) required to detect the amplified product was determined and semi-logarithmic standard plots were drawn (Ct vs cDNA amount). The calculations were performed based on the Ct method. This technique uses the formula  $2^{-\Delta\Delta Ct}$  to calculate the expression of target genes normalized to a calibrator (N° Fold). The Ct indicates the cycle number in which the amount of amplified target reaches a fixed threshold. The Ct data for all target and housekeeping genes in each sample were used to establish  $\Delta Ct$  values [ $\Delta Ct = Ct$  (target gene) –  $Ct$  (housekeeping gene)]. In our experiments,  $\beta$ -actin was used as a reference (housekeeping) gene. Thereafter,  $\Delta\Delta Ct$  values were calculated by subtracting the calibrator from the  $\Delta Ct$  value of each target. The relative quantity (RQ), or N° fold, was calculated using the equation  $RQ = 2^{-\Delta\Delta Ct}$  (Livak et al., 2001). Real-time RT-PCR data were quantified using the SDS 2.2 software package.

### Statistical analysis

Data are expressed as the mean  $\pm$  S.E.M. from at least eight samples. In all cases, data were analyzed by ANOVA followed by post-hoc Tukey-Kramer multiple-comparison tests. *P* values lower than 0.05 were considered significant.

## RESULTS

At the end of the experimental protocol, the different experimental groups registered no significant changes in weight gain (data not shown). Weekly control of food intake was performed both in control and IF mice and was on average per week of 35 g and 28 g, respectively.

Microarray analysis were performed in order to simultaneously analyze the expression of several genes involved in signaling pathways related to oxidative stress,

mitochondrial-related apoptosis, cell cycle proteins, sirtuin family, and other proteins associated with neurologic diseases, cell structure and general cell processes. Total of 62 genes were tested and the resultant z-scores were obtained from four independent experiments each performed in duplicate. Table 1 shows the list of genes included in the array and difference in levels of gene expression (z-score) between the control SAMP8 and SAMR1, whereas Table 2 shows the list of genes included in the array and differences in levels of gene score (z-score) between the SAMP8 and SAMP8 mice. Although the analysis software establishes that a z-score over 1.5 indicates a possible differentially expressed gene, on the basis of previous analysis (Rojas-Mayorquin et al., 2008) we considered only those genes with z-score over 2.0 as significant for further analysis. After cross analysis, none of the genes exceeded this value in any of the comparisons performed. However, we found some genes with a z-score of between 1.5 and 2.0 (see tables 1 and 2). For instance, in SAMP8 mice three genes exceeded a z-score of 1.5: Rb1 (-1.95), Casp9 (-1.65) and Park2 (-1.50) compared with SAMR1 mice (Table 1). On the other hand, in SAMP8 mice the expression of Gpx1 (-1.89), Jun (-1.76) and E2f1 (-1.57) were reduced and that of App increased (1.61) after intermittent fasting (Table 2). Therefore, at least at transcription level, non-significant modifications in the genes tested were induced by IF in the SAMP8 model under our experimental strategy.

As show in Fig 1A the conventional RT-PCR analysis showed a lower sirtuin 1 gene expression in IF-SAMP8 mice compared with IF-SAMP8 mice. Sirtuin 1 expression was lower in the cortex of SAMP8 than SAMR1 mice, but intermittent fasting partially recovered the sirtuin 1 protein levels of the IF-SAMP8 mice (Fig 1B). Similar results were obtained for the hippocampus (Data not shown). SAMP8 presented higher acetylated NF $\kappa$ B than SAMR1 mice. IF induced a decrease in the acetylated form of this transcription factor in SAMR1 and SAMP8. With respect to FoxO1, immunoprecipitation studies of this transcription factor indicated that, in non-fasted SAMP8 mice, the acetylated form of FoxO1 was significantly greater in SAMP8 than in SAMR1, while SAMP8 mice on the IF regimen showed a significant reduction of Ac-FoxO1 (Fig 2B).

As a measure of the neuroprotective effect of IF in ageing, we chose two well-known markers of survival, namely the neurotrophic factor BDNF and HSP70, a marker of

neuronal survival. The expression of BDNF in SAMP8 was lower than in SAMR1 mice. However, there was a significant increase in BDNF levels in IF-SAMP8 mice compared to SAMP8 mice (Fig 3A). In our experimental conditions, samples from SAMP8 mice displayed lower HSP70 expression than in SAMR1 mice. A significant recovery in HSP70 expression was noted in IF-SAMP8 mice compared with SAMP8 mice, yielding similar values to SAMR1 mice (Fig 3B).

In reference to hallmark proteins of AD, we studied the expression of p-tau Ser<sup>199</sup>, p-GSK3 $\beta$  Tyr<sup>216</sup> and ADAM10. A significant reduction in tau hyperphosphorylation in IF-SAMP8 was detected in comparison to SAMP8 mice (Fig. 4A). Accordingly, IF induced a decrease in p-GSK3 $\beta$  Tyr<sup>216</sup>, which represents the active form of this kinase (Fig. 3A). SAMP8 mice had a significantly lower expression of ADAM10 compared to SAMR1 mice; however, the expression of this protein was recovered in IF-SAMP8 mice (Fig 4B).

In addition, we studied p-FoxO1 and p-JNK as indicators of neurodegenerative processes. No changes were observed in IF-SAMR1 mice compared with SAMR1 mice, but a significant variation in p-FoxO1 and p-JNK was detected between IF-SAMP8 mice and SAMP8 mice (Fig 5), similarly to levels displayed in SAMR1 mice.

## DISCUSSION

Restricted calorie intake ameliorates senescence-related diseases such as AD and metabolic syndrome in several systems and experimental models, including humans. Moreover, increasing evidence from studies of human populations suggests that overeating and diabetes increase the risk of AD (Janson et al., 2004; Launer, 2005; Luchsinger et al., 2004; Ott et al., 1999), and that low calorie diets reduce those risks (Luchsinger et al., 2002). One variation of restricted calorie intake is intermittent fasting (IF), an experimental strategy that has some similarities to calorie reduction and is widely used to study the effects of a reduced calorie intake on organisms (Halagappa et al., 2007).

In current studies, non-significant changes were found in the transcriptional activity of the 62 genes tested. In contrast, at a phenotypic level, we found that IF ameliorated p-tau Ser<sup>199</sup> expression in SAMP8 (Canudas et al., 2005; Tajés et al., 2008), as well as

other neurodegenerative hallmarks of this strain, such as p-GSK3 $\beta$  Tyr<sup>216</sup>, p-FoxO1 and p-JNK expression (Tajes et al., 2009a). Our result corroborate the protective role of IF in this murine model, as shown by indirect markers of neuroprotection such as the higher expression of BDNF and HSP70 in IF mice (Lee et al., 2000).

Our study focused on the sirtuin 1 pathway, one of the signalling cascades implicated in the protective process. Sirtuin 1 belongs to a nicotinamide adenine dinucleotide (NAD)<sup>+</sup>-dependent protein deacetylase family of ontogenically well-conserved molecules. Sirtuin family members regulate not only gene silencing, DNA repair, and rDNA recombination, but also ageing, and apoptosis (Grubisha et al., 2005; Michan et al., 2007). In this context, increased sirtuin 1 expression protects cells against A $\beta$ -induced reactive oxygen species (ROS) production and DNA damage, thereby reducing apoptotic death *in vitro* (Alcendor et al., 2004; Kim et al., 2007). Moreover, in AD, neurons are rescued by the over-expression of sirtuin 1 induced by either CR (Mattson, 2000) or the administration of resveratrol (Vingtdeux et al., 2008), a potential activator of this enzyme.

SAMP8 show low sirtuin 1 expression and a reduced activation of this deacetylase with age (Pallas et al., 2008; Gutierrez-Cuesta et al., 2008). Accordingly, a significant reduction in sirtuin 1 activity in SAMP8 was observed in comparison to SAMR1. Interestingly, IF-SAMP8 presented an increase in sirtuin 1 expression, which reached SAMR1 values. However, we detected a slight reduction in sirtuin 1 gene expression after IF in SAMP8. It has also been described that the rise in sirtuin 6 protein expression after calorie restriction is caused by an increase in the stability of the protein and not enhanced transcription (Kanfi et al., 2008b). Recently, the same authors demonstrated that the increase in sirtuin 1 expression after fasting in mice is also due to the stabilization of protein, not an increase due to sirtuin 1 mRNA (Kanfi et al., 2008a). Our findings show that IF increases sirtuin 1 protein expression and reduces the mRNA levels in SAMP8 mice, indicating a stabilization of protein after a reduction in food intake.

In accordance with previous results (Gutierrez-Cuesta et al., 2008), SAMP8 mice presented higher acetylated NF $\kappa$ B than SAMR1 mice. As a result of the increase in sirtuin 1 protein expression, some of the protein's targets, such as NF $\kappa$ B or FoxO1, were more deacetylated in IF-SAMP8 than in control SAMP8 mice. These results

correlate with an increase in pro-survival signals or factors, such as BDNF or HSP70. The relationship between BDNF, HSP70 and sirtuin 1 has been described in several neuronal systems. For example, neurotrophic factors protect neurons in several experimental models of neurodegenerative disorders. Moreover, the expression of several neurotrophic factors, the most notable of which is BDNF, increases in the brain of rats and mice on a calorie restriction regimen (Duan et al., 2001; Lee et al., 2000) while infusion of a BDNF blocking antibody into the lateral ventricles of rats on a restricted diet significantly attenuates the protective effect (Lee et al., 2002).

SAMP8 mice display a reduction in ADAM10 expression concomitantly with an increase in oligomeric amyloid deposition in the brain. After IF, the ADAM10 protein increased in SAMP8 mice, thereby corroborating the previously described relationship between sirtuin 1 and ADAM10 through mechanisms involving the regulation of the serine/threonine Rho kinase ROCK1 (Qin et al., 2006a). Firm evidence of this relationship was obtained when Patel (Patel et al., 2005) showed that short-term calorie restriction substantially decreased the accumulation of A $\beta$  plaques in two AD-prone APP/presenilin transgenic mouse lines, and decreased the presence of gliosis marked by astrocytic activation. In another study, Qin and colleagues (Qin et al., 2006b) showed that a restricted dietary regimen prevents A $\beta$  peptide generation and neuritic plaque deposition in the brain of another AD mouse model (Tg2576 mice). In a recent report, the same group showed that calorie restriction results in reduced A $\beta$  content in the temporal cortex of squirrel monkeys, in a manner that was inversely correlated with sirtuin 1 protein concentrations in the same brain region (Qin et al., 2006a).

To ascertain the beneficial effects of IF in SAMP8, we studied several apoptotic pathways in this senescence model. Among other cellular systems controlling senescence, we examined JNK and FoxO1 signaling by phosphorylation because these transcription factors are implicated in cellular demise. In the present study, we demonstrate that IF in SAMP8 recovery the phosphorylated levels of these two factors to SAMR1, thereby indicating that an IF regimen promotes a neuroprotective effect, which is possibly additive to sirtuin 1 activation. In addition, IF results in a decrease in GSK3 $\beta$  activation and tau phosphorylation in SAMP8, hence possibly reducing neurofibrillar tangle formation and neuronal death, as described elsewhere (Tajes et al., 2008; Canudas et al., 2005).

In conclusion, IF activated the sirtuin 1 pathway, a critical signaling cascade involved in longevity and cellular health in the senescence-accelerated model used in this study. Moreover, this dietary regimen reduced some of the death signals implicated in neuronal death and ageing processes. These findings corroborate the results of other authors using distinct animal senescence models or other dietary/pharmacological strategies to activate the sirtuin 1 pathway. Our data indicate that dietary strategies or the modulation of the cellular system could provide potential approaches to slow the ageing process, thereby reducing frailty and improving health in old age.

### ACKNOWLEDGEMENTS

We thank the Language Advisory Service of the University of Barcelona for revising the manuscript. This study was supported by grants SAF-2009-13093 from the “Ministerio de Educación y Ciencia”, PI080400 from the “Instituto de Salud Carlos III”, 2009/SGR00893 from the “Generalitat de Catalunya” and 0310 from the “Fundació La Marató de TV3”.

### REFERENCES

1. Alcendor, R. R., Kirshenbaum, L. A., Imai, S., Vatner, S. F., Sadoshima, J. 2004. Silent information regulator 2alpha, a longevity factor and class III histone deacetylase, is an essential endogenous apoptosis inhibitor in cardiac myocytes. *Circ.Res.* 95, 971-980.
2. Calabrese, V., Cornelius, C., Mancuso, C., Pennisi, G., Calafato, S., Bellia, F., Bates, T. E., Giuffrida Stella, A. M., Schapira, T., Ankova Kostova, A. T., Rizzarelli, E. 2008. Cellular stress response: a novel target for chemoprevention and nutritional neuroprotection in aging, neurodegenerative disorders and longevity. *Neurochem.Res.* 33, 2444-2471.
3. Canudas, A. M., Gutierrez-Cuesta, J., Rodriguez, M. I., Acuna-Castroviejo, D., Sureda, F. X., Camins, A., Pallas, M. 2005. Hyperphosphorylation of microtubule-associated protein tau in senescence-accelerated mouse (SAM). *Mech.Ageing Dev.* 126, 1300-1304.

4. Duan, W., Lee, J., Guo, Z., Mattson, M. P. 2001. Dietary restriction stimulates BDNF production in the brain and thereby protects neurons against excitotoxic injury. *J.Mol.Neurosci* 16, 1-12.
5. Gómez-Mayen, A. C.-G. G. R.-R. L. C.-C. G. The Package "GenArise" (API) Version 1.7.3 Microarray analysis tool. <http://www.ifc.unam.mx/genarise/>. 2006.
6. Grubisha, O., Smith, B. C., Denu, J. M. 2005. Small molecule regulation of Sir2 protein deacetylases. *FEBS J.* 272, 4607-4616.
7. Gutierrez-Cuesta, J., Tajés, M., Jimenez, A., Coto-Montes, A., Camins, A., Pallas, M. 2008. Evaluation of potential pro-survival pathways regulated by melatonin in a murine senescence model. *J.Pineal Res.* 45, 497-505.
8. Halagappa, V. K., Guo, Z., Pearson, M., Matsuoka, Y., Cutler, R. G., LaFerla, F. M., Mattson, M. P. 2007. Intermittent fasting and caloric restriction ameliorate age-related behavioral deficits in the triple-transgenic mouse model of Alzheimer's disease. *Neurobiol.Dis.* 26, 212-220.
9. Hipkiss, A. R. 2007. Dietary restriction, glycolysis, hormesis and ageing. *Biogerontology.* 8, 221-224.
10. Janson, J., Laedtke, T., Parisi, J. E., O'Brien, P., Petersen, R. C., Butler, P. C. 2004. Increased risk of type 2 diabetes in Alzheimer disease. *Diabetes* 53, 474-481.
11. Kanfi, Y., Peshti, V., Gozlan, Y. M., Rathaus, M., Gil, R., Cohen, H. Y. 2008a. Regulation of SIRT1 protein levels by nutrient availability. *FEBS Lett.* 582, 2417-2423.
12. Kanfi, Y., Shalman, R., Peshti, V., Pilosof, S. N., Gozlan, Y. M., Pearson, K. J., Lerrer, B., Moazed, D., Marine, J. C., de, C. R., Cohen, H. Y. 2008b. Regulation of SIRT6 protein levels by nutrient availability. *FEBS Lett.* 582, 543-548.
13. Kim, D., Nguyen, M. D., Dobbin, M. M., Fischer, A., Sananbenesi, F., Rodgers, J. T., Delalle, I., Baur, J. A., Sui, G., Armour, S. M., Puigserver, P., Sinclair, D. A., Tsai, L. H. 2007. SIRT1 deacetylase protects against neurodegeneration in models for Alzheimer's disease and amyotrophic lateral sclerosis. *EMBO J.* 26, 3169-3179.
14. Komatsu, T., Chiba, T., Yamaza, H., Yamashita, K., Shimada, A., Hoshiyama, Y., Henmi, T., Ohtani, H., Higami, Y., de, C. R., Ingram, D. K., Shimokawa, I.

2008. Manipulation of caloric content but not diet composition, attenuates the deficit in learning and memory of senescence-accelerated mouse strain P8. *Exp.Gerontol.*
15. Launer, L. J. 2005. Diabetes and brain aging: epidemiologic evidence. *Curr.Diab.Rep.* 5, 59-63.
  16. Lee, J., Duan, W., Long, J. M., Ingram, D. K., Mattson, M. P. 2000. Dietary restriction increases the number of newly generated neural cells, and induces BDNF expression, in the dentate gyrus of rats. *J.Mol.Neurosci* 15, 99-108.
  17. Lee, J., Duan, W., Mattson, M. P. 2002. Evidence that brain-derived neurotrophic factor is required for basal neurogenesis and mediates, in part, the enhancement of neurogenesis by dietary restriction in the hippocampus of adult mice. *J.Neurochem.* 82, 1367-1375.
  18. Livak, K. J., Schmittgen, T. D. 2001. Analysis of relative gene expression data using real-time quantitative PCR and the 2(-Delta Delta C(T)) Method. *Methods* 25, 402-408
  19. Luchsinger, J. A., Tang, M. X., Shea, S., Mayeux, R. 2004. Hyperinsulinemia and risk of Alzheimer disease. *Neurology* 63, 1187-1192.
  20. Luchsinger, J. A., Tang, M. X., Shea, S., Mayeux, R. 2002. Caloric intake and the risk of Alzheimer disease. *Arch.Neurol.* 59, 1258-1263.
  21. Martin, B., Mattson, M. P., Maudsley, S. 2006. Caloric restriction and intermittent fasting: two potential diets for successful brain aging. *Ageing Res.Rev.* 5, 332-353.
  22. Mattson, M. P. 2000. Existing data suggest that Alzheimer's disease is preventable. *Ann.N.Y.Acad.Sci.* 924, 153-159.
  23. Mattson, M. P. 2003. Will caloric restriction and folate protect against AD and PD? *Neurology* 60, 690-695.
  24. Mattson, M. P., Duan, W., Chan, S. L., Cheng, A., Haughey, N., Gary, D. S., Guo, Z., Lee, J., Furukawa, K. 2002. Neuroprotective and neurorestorative signal transduction mechanisms in brain aging: modification by genes, diet and behavior. *Neurobiol.Aging* 23, 695-705.
  25. Michan, S., Sinclair, D. 2007. Sirtuins in mammals: insights into their biological function. *Biochem.J.* 404, 1-13.



26. Ott, A., Stolk, R. P., van, H. F., Pols, H. A., Hofman, A., Breteler, M. M. 1999. Diabetes mellitus and the risk of dementia: The Rotterdam Study. *Neurology* 53, 1937-1942.
27. Pallas, M., Pizarro, J. G., Gutierrez-Cuesta, J., Crespo-Biel, N., Alvira, D., Tajés, M., Yeste-Velasco, M., Folch, J., Canudas, A. M., Sureda, F. X., Ferrer, I., Camins, A. Modulation of SIRT1 expression in different neurodegenerative models and human pathologies. *Neuroscience*. 2008.
28. Patel, N. V., Gordon, M. N., Connor, K. E., Good, R. A., Engelman, R. W., Mason, J., Morgan, D. G., Morgan, T. E., Finch, C. E. 2005. Caloric restriction attenuates Abeta-deposition in Alzheimer transgenic models. *Neurobiol.Aging* 26, 995-1000.
29. Qin, W., Chachich, M., Lane, M., Roth, G., Bryant, M., de, C. R., Ottinger, M. A., Mattison, J., Ingram, D., Gandy, S., Pasinetti, G. M. 2006a. Calorie restriction attenuates Alzheimer's disease type brain amyloidosis in Squirrel monkeys (*Saimiri sciureus*). *J.Alzheimers.Dis.* 10, 417-422.
30. Qin, W., Yang, T., Ho, L., Zhao, Z., Wang, J., Chen, L., Zhao, W., Thiagarajan, M., MacGrogan, D., Rodgers, J. T., Puigserver, P., Sadoshima, J., Deng, H., Pedrini, S., Gandy, S., Sauve, A. A., Pasinetti, G. M. 2006b. Neuronal SIRT1 activation as a novel mechanism underlying the prevention of Alzheimer disease amyloid neuropathology by calorie restriction. *J.Biol.Chem.* 281, 21745-21754.
31. Rodgers, J. T., Lerin, C., Haas, W., Gygi, S. P., Spiegelman, B. M., Puigserver, P. 2005. Nutrient control of glucose homeostasis through a complex of PGC-1alpha and SIRT1. *Nature* 434, 113-118.
32. Rojas-Mayorquin, A. E., Torres-Ruiz, N. M., Ortuno-Sahagun, D., Gudino-Cabrera, G. 2008. Microarray analysis of striatal embryonic stem cells induced to differentiate by ensheathing cell conditioned media. *Dev.Dyn.* 237, 979-994.
33. Salminen, A., Ojala, J., Huuskonen, J., Kauppinen, A., Suuronen, T., Kaarniranta, K. 2008. Interaction of aging-associated signaling cascades: inhibition of NF-kappaB signaling by longevity factors FoxOs and SIRT1. *Cell Mol.Life Sci.* 65, 1049-1058.
34. Smith, J. 2002. Human Sir2 and the 'silencing' of p53 activity. *Trends Cell Biol.* 12, 404-406.

35. Tajés, M., Gutierrez-Cuesta, J., Folch, J., Ferrer, I., Caballero, B., Smith, M. A., Casadesus, G., Camins, A., Pallas, M. 2008. Lithium treatment decreases activities of tau kinases in a murine model of senescence. *J.Neuropathol.Exp.Neurol.* 67, 612-623.
36. Tajés, M., Yeste-Velasco, M., Zhu, X., Chou, S. P., Smith, M. A., Pallas, M., Camins, A., Casadesus, G. 2009a. Activation of Akt by lithium: pro-survival pathways in aging. *Mech.Ageing Dev.* 130, 253-261.
37. Takeda, T. 1999. Senescence-accelerated mouse (SAM): a biogerontological resource in aging research. *Neurobiol.Aging* 20, 105-110.
38. Vingtdoux, V., Dreses-Werringloer, U., Zhao, H., Davies, P., Marambaud, P. 2008. Therapeutic potential of resveratrol in Alzheimer's disease. *BMC.Neurosci* 9 Suppl 2, S6.
39. Wang, F., Nguyen, M., Qin, F. X., Tong, Q. 2007. SIRT2 deacetylates FOXO3a in response to oxidative stress and caloric restriction. *Aging Cell* 6, 505-514.
40. Westphal, C. H., Dipp, M. A., Guarente, L. 2007. A therapeutic role for sirtuins in diseases of aging? *Trends Biochem.Sci.* 32, 555-560.

### Figure legends

Fig 1: (A) Semi-quantitative RT-PCR analysis of sirtuin 1 mRNA in cortex of SAMR1 and SAMP8 mice non-fasted (CT R1 and CT P8) and after intermittent fasting (IF R1 and IF P8). (B) Sirtuin 1 expression in the experimental conditions tested. Sirtuin 1 expression increased in IF-SAMP8 mice compared with SAMP8 mice. Images show representative Western blot and bar graph obtained from semi-quantitative image analysis, as described in *Materials and methods*. Data represent means  $\pm$  SD of 6-8 mice. \*\*\* $p < 0.001$  vs. CT R1; ## $p < 0.01$  vs. CT P8

Fig 2: Protein expression of Ac-NF $\kappa$ B (A) and Ac-FoxO1 (B) in cortex of SAMR1 and SAMP8 mice non-fasted (CT R1 and CT P8) and after intermittent fasting (IF R1 and IF P8). Results showed that Ac-NF $\kappa$ B and Ac-FoxO1 expression in IF P8 are lower than in CT P8. Images showed representative Western blot and bar graph obtained from semi-quantitative image analysis, as described in *Materials and methods*. Data

represent means  $\pm$  SD of 6-8 mice. \* $p < 0.05$ , \*\* $p < 0.01$  and \*\*\* $p < 0.001$  vs. CT R1; ### $p < 0.001$  vs. CT P8.

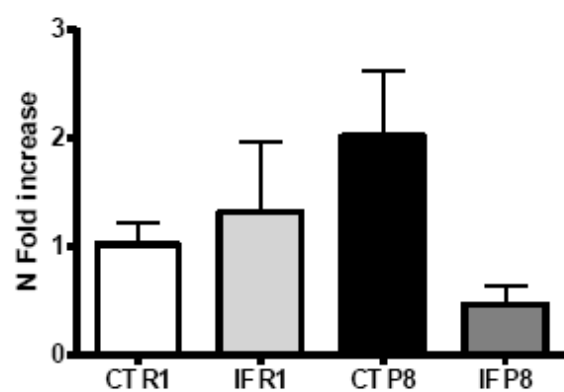
Fig 3: BDNF and HSP70 expression in cortex of SAMR1 and SAMP8 mice non-fasted (CT R1 and CT P8) and after intermittent fasting (IF R1 and IF P8). (A) BDNF expression in CT P8 was significantly lower than in CT R1. IF treatment restored the expression of this neurotrophic factor. (B) HSP70 presented a similar recovery profile than BDNF after IF in CT P8. Images show representative Western blot and bar graph obtained from semi-quantitative image analysis as mentioned in *Materials and methods*. Data represent means  $\pm$  SD of 6-8 mice. \*\* $p < 0.01$  vs. CT R1; # $p < 0.05$ ; ### $p < 0.001$  vs. CT P8.

Fig 4. (A) The degree of Tau phosphorylation in Ser<sup>199</sup> was higher in CT P8 than in IF-P8, concomitantly a higher p-GSK3 $\beta$  Tyr<sup>216</sup> activation. IF reduced phosphorylations in SAMP-8 (B) ADAM10 levels in CT R1 are higher than in P8. Results showed that IF-P8 recovered ADAM10 to CT R1 levels. Images show representative Western blot and bar graph obtained from semi-quantitative image analysis, as described in *Materials and methods*. Data represent means  $\pm$  SD of 6-8 mice. \*\* $p < 0.01$ ; \*\*\* $p < 0.001$  vs. CT R1; ## $p < 0.01$ ; ### $p < 0.001$  vs. CT P8.

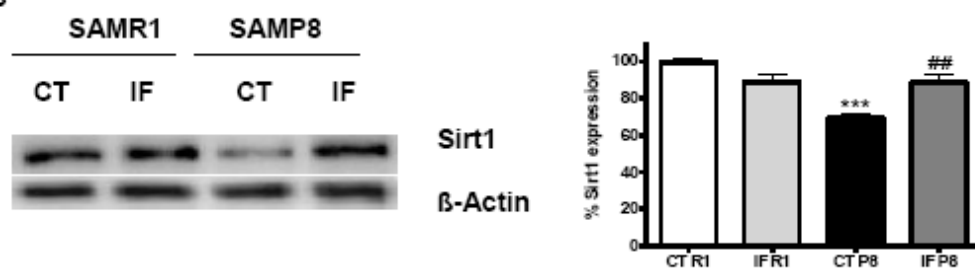
Fig. 5. p-FoxO1 and p-JNK expression in cortex of SAMR1 and SAMP8 mice non-fasted (CT R1 and CT P8) and after intermittent fasting (IF R1 and IF P8) (A) Expression of p-FoxO1 in IFP8 was significantly higher than in CT P8. (B) p-JNK showed a reduction in the phosphorylated form in IF compared with CT P8. Images show representative Western blot, and bar graph obtained from semi-quantitative image analysis, as described in *Materials and methods*. Data represent means  $\pm$  SD of 6-8 mice. \*\*\* $p < 0.001$  vs. CT R1; ## $p < 0.01$ ; ### $p < 0.001$  vs. CT P8

Tajes et al Figure 1

A



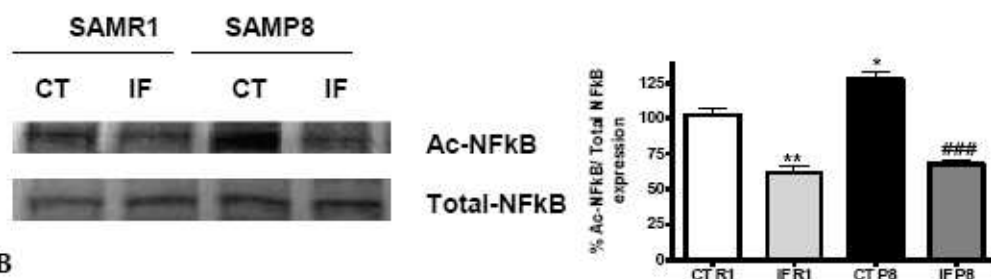
B



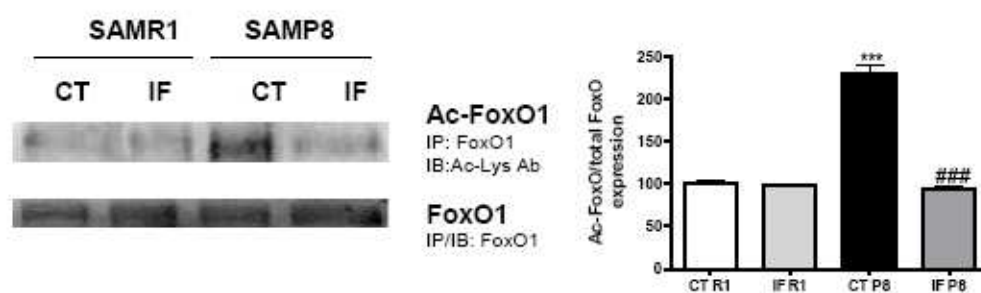
AC

Tajes et al Figure 2

A

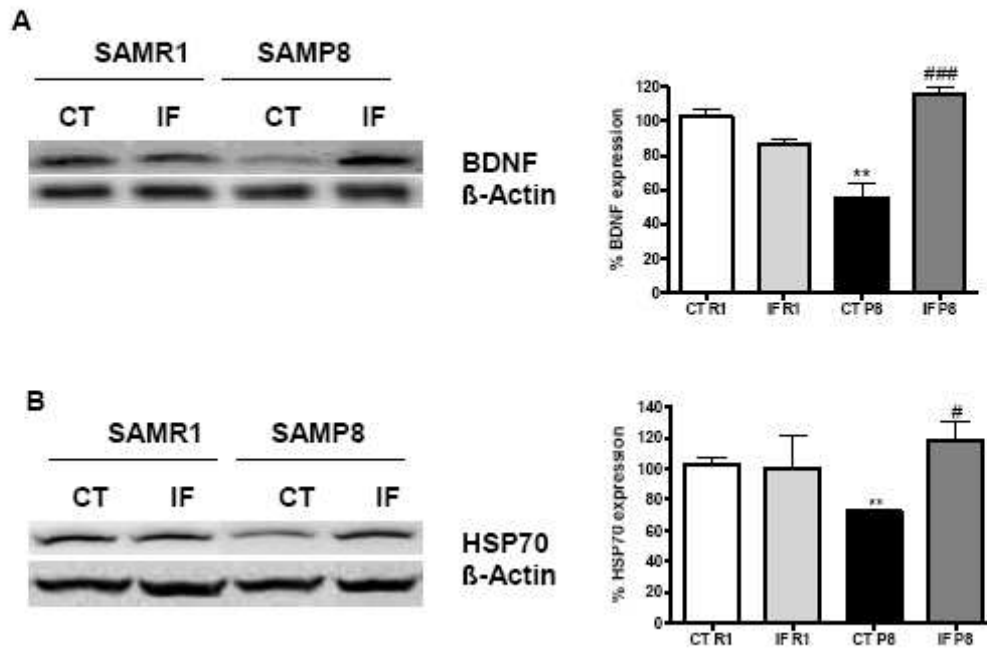


B



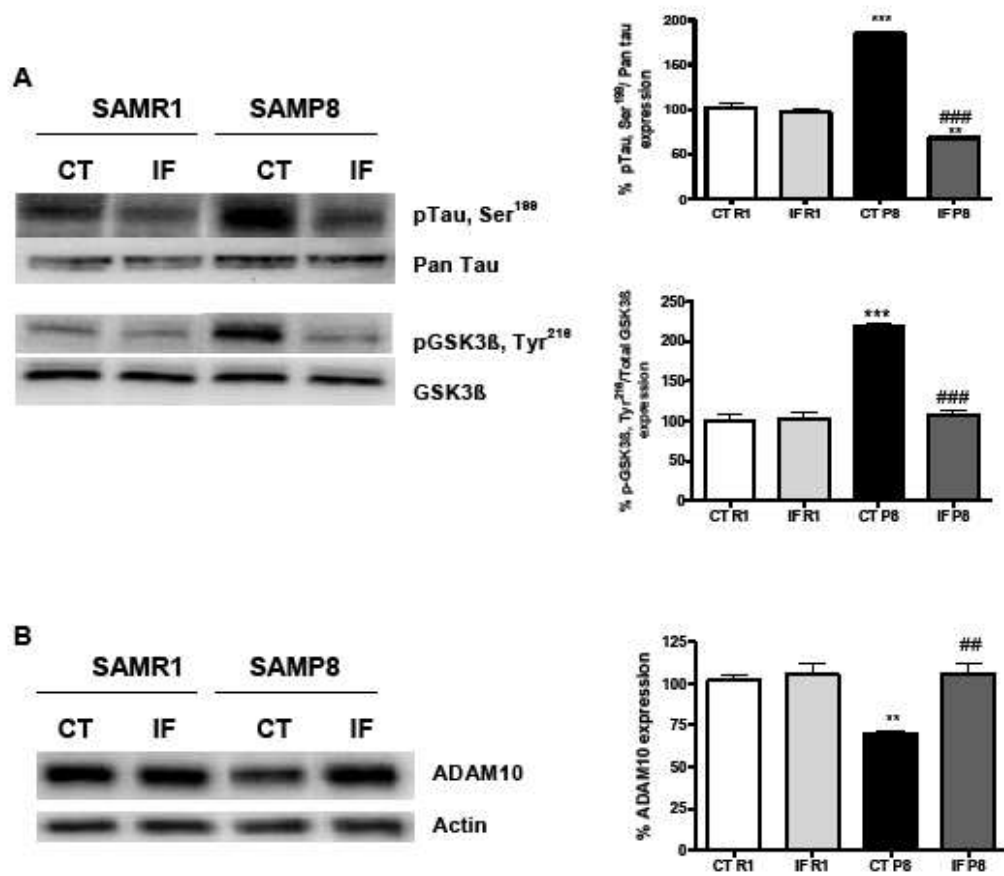
ACCEPTED

Tajes et al. Figure 3



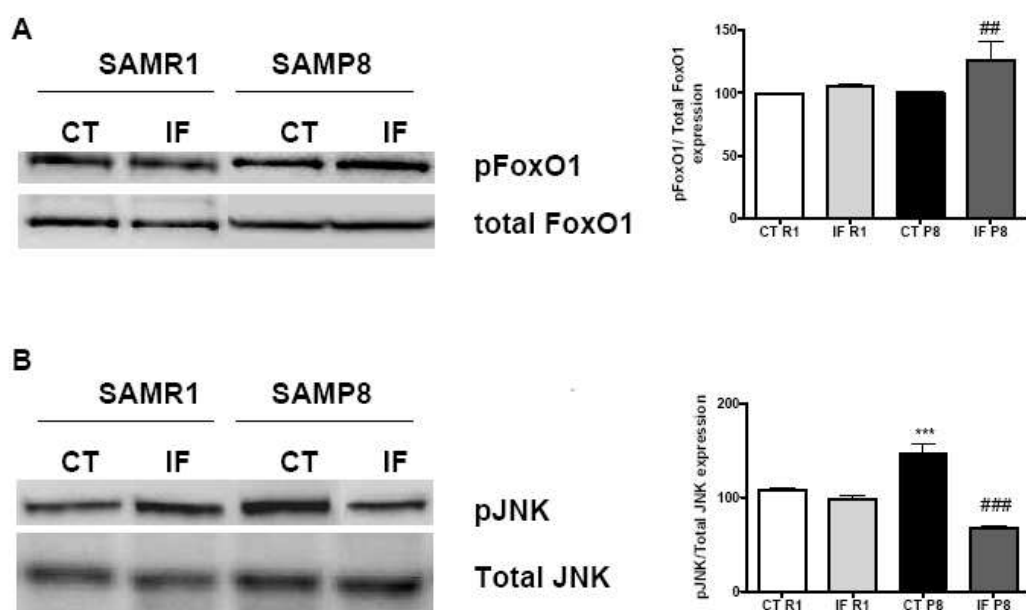
ACCEPTED

Tajes et al., Figure 4



ACCEPTED

Tajes et al., Figure 5



ACCEPTED



**Table 1. List of genes included in the array and z-score of the gen expression levels between SAMP8 and SAMR1. n.d. No determined.**

GENE ID	Symbol	Gene name	z-score	GENE ID	Symbol	Gene name	z-score
NM_009029	Rb1	retinoblastoma 1	-1.95	NM_008084	Gapdh	glyceraldehyde-3-phosphate dehydrogenase	0.00
NM_015733	Casp9	caspase 9	-1.65	NM_008639	Mtnr1a	melatonin receptor 1A	0.01
NM_016694	Park2	parkin	-1.50	NM_009870	Cdk4	cyclin-dependent kinase 4	0.04
NM_012019	Aifm1	apoptosis-inducing factor, mitochondrion-associated 1	-1.38	NM_009983	Ctsd	cathepsin D	0.11
NM_009875	Cdkn1b	cyclin-dependent kinase inhibitor 1B	-1.33	NM_019584	Becn1	beclin 1	0.18
NM_007891	E2f1	E2F transcription factor 1	-1.00	NM_007393	Actb	actin, beta, cytoplasmic	0.21
NM_007631	Ccnd1	cyclin D1	-0.92	NM_007600	Capn1	calpain 1	0.22
NM_007471	App	amyloid beta (A4) precursor protein	-0.90	NM_001038609	Mapt	microtubule-associated protein tau, transcript variant 1	0.27
NM_009812	Casp8	caspase 8, transcript variant 1	-0.88	NM_009656	Aldh2	aldehyde dehydrogenase 2, mitochondrial	0.30
NM_007614	Ctnnb1	catenin (cadherin associated protein), beta 1	-0.70	NM_183417	Cdk2	cyclin-dependent kinase 2 transcript variant 1	0.31
NM_181586	Sirt6	sirtuin 6 (silent mating type information regulation 2, homolog) 6	-0.66	NM_019739	Foxo1	forkhead box O1	0.32
NM_010279	Gfra1	glial cell line derived neurotrophic factor family receptor alpha 1	-0.57	NM_013671	Sod2	superoxide dismutase 2, mitochondrial	0.34
NM_009871	Cdk5r1	cyclin-dependent kinase 5, regulatory subunit (p35) 1	-0.53	NM_007628	Ccna1	cyclin A1	0.34
NM_011949	Mapk1	mitogen activated protein kinase 1, transcript	-0.44	NM_007527	Bax	Bcl2-associated X protein	0.38
NM_011045	Pcna	proliferating cell nuclear antigen	-0.42	NM_025735	Map1lc3	microtubule-associated protein 1 light chain 3 alpha	0.43
NM_007545	Hrk	harakiri, BCL2 interacting protein (contains only BH3 domain)	-0.41	NM_007668	Cdk5	cyclin-dependent kinase 5	0.46
NM_008730	Nptx1	neuronal pentraxin 1	-0.39	NM_010065	Dnm1	dynamain 1	0.47

NM_019740	Foxo3a	forkhead box O3a	-0.38	NM_009810	Casp3	caspase 3	0.50
NM_009804	Cat	catalase	-0.35	NM_010362	Gsto1	glutathione S-transferase omega 1	0.50
NM_019639	Ubc	ubiquitin C	-0.31	NM_178848	Sirt5	sirtuin 5 (silent mating type information regulation 2 homolog) 5	0.52
NM_022432	Sirt2	sirtuin 2 (silent mating type information regulation 2, homolog) 2	-0.30	NM_011144	Ppara	peroxisome proliferator activated receptor alpha	0.59
NM_133828	Creb1	cAMP responsive element binding protein 1, transcript variant A	-0.25	NM_011640	Trp53	transformation related protein 53	0.62
NM_019827	Gsk3b	glycogen synthase kinase 3 beta	-0.20	NM_009050	Ret	ret proto-oncogene, transcript variant 2	0.64
NM_019812	Sirt1	sirtuin 1 (silent mating type information regulation 2, homolog) 1	-0.17	NM_007544	Bid	BH3 interacting domain death agonist	0.66
NM_008160	Gpx1	glutathione peroxidase 1	-0.15	NM_019467	Aif1	allograft inflammatory factor 1	0.67
NM_010344	Gsr	glutathione reductase 1	-0.15	NM_011952	Mapk3	Mitogen activated protein kinase 3	0.71
XM_991632	Sirt4	sirtuin 4 (silent mating type information regulation 2 homolog) 4	-0.10	NM_153056	Sirt7	sirtuin 7 (silent mating type information regulation 2, homolog) 7	0.90
NM_022433	Sirt3	sirtuin 3 (silent mating type information regulation 2, homolog) 3	-0.05	NM_007499	Atm	ataxia telangiectasia mutated homolog (human)	n.d
NM_009794	Capn2	calpain 2	-0.03	NM_010275	Gdnf	glial cell line derived neurotrophic factor	n.d
NM_009652	Akt1	thymoma viral proto-oncogene 1	-0.02	NM_010591	Jun	Jun oncogene	n.d
NM_009463	Ucp1	uncoupling protein 1 (mitochondrial, proton carrier)	-0.02	NM_001025074	Ntrk2	neurotrophic tyrosine kinase, receptor, type 2, transcript variant 1	n.d

**Table 2. List of genes included in the array and z-score of the gen expression levels between CT SAMP8 and IF SAMP8.**

GENE ID	Symbol	Gene name	z-score	GENE ID	Symbol	Gene name	z-score
NM_008160	Gpx1	glutathione peroxidase 1	-1.89	NM_009463	Ucp1	uncoupling protein 1 (mitochondrial, proton carrier)	-0.03
NM_010591	Jun	Jun oncogene	-1.76	NM_019467	Aif1	allograft inflammatory factor 1	-0.03
NM_007891	E2f1	E2F transcription factor 1	-1.57	NM_009794	Capn2	calpain 2	0.02
NM_011045	Pcna	proliferating cell nuclear antigen	-0.84	NM_022433	Sirt3	sirtuin 3 (silent mating type information regulation 2, homolog) 3	0.03
NM_010275	Gdnf	glial cell line derived neurotrophic factor	-0.78	NM_019639	Ubc	ubiquitin C	0.12
NM_007631	Ccnd1	cyclin D1	-0.67	NM_009804	Cat	catalase	0.13
NM_009871	Cdk5r1	cyclin-dependent kinase 5, regulatory subunit (p35) 1	-0.57	NM_013671	Sod2	superoxide dismutase 2, mitochondrial	0.13
NM_012019	Aifm1	apoptosis-inducing factor, mitochondrion-associated 1	-0.56	NM_001038609	Mapt	microtubule-associated protein tau, transcript variant 1	0.17
NM_007393	Actb	actin, beta, cytoplasmic	-0.48	NM_009810	Casp3	caspase 3	0.21
NM_181586	Sirt6	sirtuin 6 (silent mating type information regulation 2, homolog) 6	-0.47	NM_010065	Dnm1	dynamamin 1	0.22
NM_025735	Map1lc3	microtubule-associated protein 1 light chain 3 alpha	-0.47	NM_007668	Cdk5	cyclin-dependent kinase 5	0.24
NM_015733	Casp9	caspase 9	-0.41	NM_008639	Mtnr1a	melatonin receptor 1A	0.24
NM_010362	Gsto1	glutathione S-transferase omega 1	-0.35	NM_011952	Mapk3	Mitogen activated protein kinase 3	0.27
NM_019739	Foxo1	forkhead box O1	-0.34	NM_178848	Sirt5	sirtuin 5 (silent mating type information regulation 2 homolog) 5	0.31
NM_009870	Cdk4	cyclin-dependent kinase 4	-0.33	NM_019584	Becn1	beclin 1	0.31
NM_133828	Creb1	cAMP responsive element binding protein 1, transcript variant A	-0.30	NM_008730	Nptx1	neuronal pentraxin 1	0.32
NM_007545	Hrk	harakiri, BCL2 interacting protein (contains only BH3 domain)	-0.23	NM_007628	Ccna1	cyclin A1	0.43

NM_008084	Gapdh	glyceraldehyde-3-phosphate dehydrogenase	-0.18
NM_007600	Capn1	calpain 1	-0.16
NM_019740	Foxo3a	forkhead box O3a	-0.16
NM_009812	Casp8	caspase 8, transcript variant 1	-0.15
NM_009983	Ctsd	cathepsin D	-0.14
NM_153056	Sirt7	sirtuin 7 (silent mating type information regulation 2, homolog) 7	-0.13
NM_007527	Bax	Bcl2-associated X protein	-0.12
NM_010344	Gsr	glutathione reductase 1	-0.10
NM_001025074	Ntrk2	neurotrophic tyrosine kinase, receptor, type 2, transcript variant 1	-0.09
XM_991632	Sirt4	sirtuin 4 (silent mating type information regulation 2 homolog) 4	-0.08
NM_009029	Rb1	retinoblastoma 1	-0.08
NM_019827	Gsk3b	glycogen synthase kinase 3 beta	-0.07
NM_009656	Aldh2	aldehyde dehydrogenase 2, mitochondrial	-0.06
NM_022432	Sirt2	sirtuin 2 (silent mating type information regulation 2, homolog) 2	-0.05

NM_010279	Gfra1	glial cell line derived neurotrophic factor family receptor alpha 1	0.44
NM_007544	Bid	BH3 interacting domain death agonist	0.45
NM_016694	Park2	parkin	0.50
NM_009652	Akt1	thymoma viral proto-oncogene 1	0.54
NM_011949	Mapk1	mitogen activated protein kinase 1, transcript	0.56
NM_183417	Cdk2	cyclin-dependent kinase 2 transcript variant 1	0.56
NM_007499	Atm	ataxia telangiectasia mutated homolog (human)	0.57
NM_011144	Ppara	peroxisome proliferator activated receptor alpha	0.58
NM_019812	Sirt1	sirtuin 1 (silent mating type information regulation 2, homolog) 1	0.67
NM_011640	Trp53	transformation related protein 53	1.07
NM_007471	App	amyloid beta (A4) precursor protein	1.61
NM_009875	Cdkn1b	cyclin-dependent kinase inhibitor 1B	n.d
NM_007614	Ctnnb1	catenin (cadherin associated protein), beta 1	n.d
NM_009050	Ret	ret proto-oncogene, transcript variant 2	n.d